Hysteresis and magnetocaloric effect at the magnetostructural phase transition of Ni-Mn-Ga and Ni-Mn-Co-Sn Heusler alloys

Vittorio Basso and Carlo P. Sasso
Istituto Nazionale di Ricerca Metrologica, Strada delle Cacce 91, I-10135 Torino, Italy

Konstantin P. Skokov and Oliver Gutfleisch
Institute for Metallic Materials, Leibniz Institute for Solid State and Materials Research Dresden (IFW Dresden), D-01171 Dresden, Germany

Vladimir V. Khovaylo
National University of Science and Technology MISiS, Moscow 119049, Russia

(Received 2 August 2011; revised manuscript received 10 January 2012; published 24 January 2012)

Hysteresis features of the direct and inverse magnetocaloric effect associated with first-order magnetostructural phase transitions in Ni-Mn-X (X = Ga, Sn) Heusler alloys have been disclosed by differential calorimetry measurements performed either under a constant magnetic field, H, or by varying H in isothermal conditions. We have shown that the magnetocaloric effect in these alloys crucially depends on the employed measuring protocol. Experimentally observed peculiarities of the magnetocaloric effect have been explained in the framework of a model that accounts for different contributions to the Gibbs energy of austenitic g_A and martensitic g_M phases. Obtained experimental results have been summarized by plotting a phase fraction of the austenite x_A versus the driving force $g_M - g_A$. The developed approach allows one to predict reversible and irreversible features of the direct as well as inverse magnetocaloric effect in a variety of materials with first-order magnetic phase transitions.

DOI: 10.1103/PhysRevB.85.014430 PACS number(s): 75.30.Sg, 64.70.K−, 05.70.Fh

I. INTRODUCTION

Materials with a coupled magnetostructural first-order phase transition may display an enhanced magnetocaloric effect (MCE) due to the presence of the latent heat of the structural transformation.[1] This effect, called the giant magnetocaloric effect, is of a great interest for the development of magnetic refrigeration at room temperature.[2] Among the alloys displaying coupled magnetostructural transitions, we find Gd-Si-Ge,[3] La-Fe-Si,[4] Mn-Fe-P-As[5] and the family of the Heusler alloys like Ni-Mn-Ga[6–8] and Ni-Mn-Sn,[9,10] which displays a martensitic phase transformation.

The Heusler alloys are particularly attractive as magnetic refrigerant because (i) they are characterized by a large entropy change at the transformation (around $\Delta s = 30\ \mathrm{J\,kg^{-1}\,K^{-1}}$), (ii) they contain no expensive rare earths elements, and (iii) the martensitic transformation temperature, T_t, can easily be tuned around room temperature by element substitution in off-stoichiometric compounds.[1] On the other hand, martensitic transformations have the disadvantage of displaying thermal and magnetic hysteresis. The magnetic-field-induced entropy change, $\Delta s(H,T)$, around T_t is characterized by irreversibility and hysteresis[11,12] and it is not yet clear how it is possible to achieve, by a magnetic field, the full entropy change available at the first-order transformation.[9,12] The MCE depends on the magnetic and thermal history of the system and the hysteresis of the phase transformation is the feature that generates the irreversibility effects.[11,13,14]

The aim of the present paper is to establish quantitative relations between the measured irreversibility of MCE and the hysteresis of the first-order phase transition. For the present study two representatives of the Heusler alloys with relevant MCE and relatively *small* and *large* hysteresis were selected. The sample with relatively *small* hysteresis is $Ni_{53.3}Mn_{20.1}Ga_{26.6}$ single crystal, while the sample with relatively *large* hysteresis is $Ni_{50}Mn_{36}Co_1Sn_{13}$ polycrystal. The Ni-Mn-Ga-based alloys exhibit conventional MCE, due to a common transformation sequence from a low-temperature ferromagnetic martensitic state to a high-temperature paramagnetic (or ferromagnetic) austenite. For these alloys the magnetic-field-induced entropy change, Δs, in the vicinity of the martensitic transformation temperature, T_t, is negative because the magnetic field stabilizes the low-temperature phase with a higher magnetization.[6–8] Contrary to Ni-Mn-Ga, an uncommon transformation from the low-temperature paramagnetic to the high-temperature ferromagnetic state can be realized in Ni-Mn-Co-Sn alloys with certain composition. In this case, Δs around T_t is positive and the system exhibits so-called inverse MCE.[9,10]

II. MATERIALS AND THE MEASUREMENT PROCEDURE

Ni-Mn-Ga *with direct MCE*. Some Ni-Mn-Ga alloys display a coupled magnetostructural transition between the magnetically ordered martensite (M) and the paramagnetic austenite (A) and are characterized by a direct MCE around the transition. Typical behavior of the spontaneous magnetization is sketched in the left side of Fig. 1, with $T_{c_A} < T_{c_M}$. According to the phase diagram reported in Ref. 6 the stoichiometric compound Ni_2MnGa has $T_t < T_{c_A}$ with $T_t = 202$ K and $T_{c_A} = 376$ K. The off-stoichiometric compound $Ni_{2+x}Mn_{1-x}Ga$, with Mn partially substituted by Ni, displays an increase of T_t and a decrease of T_{c_A} with increasing x. The crossing of the two temperatures is observed for a Ni excess around $x = 0.19$ and for this composition the transformation from ferromagnetic martensite to paramagnetic austenite takes place at $T_t = 342$ K. The type of transition where $T_{c_A} < T_t < T_{c_M}$

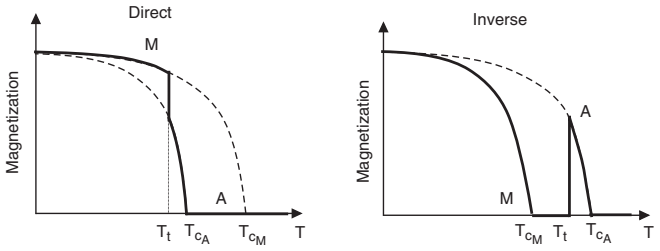

FIG. 1. Scheme of the temperature dependence of spontaneous magnetization at the martensitic transformation in Heusler alloys. (Left) Material with a direct MCE like Ni-Mn-Ga. (Right) Material with an inverse MCE like Ni-Mn-Sn.

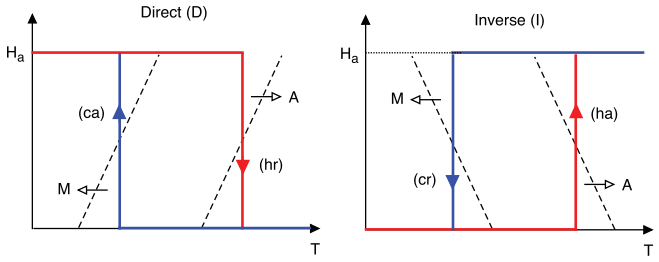

FIG. 2. (Color online) Schematic phase diagrams for materials with direct (D) and inverse (I) magnetocaloric effect. The dashed lines represents the hysteretic thresholds for the transition from A to M and from M to A. The measuring protocols heat-remove (hr) and cool-apply (ca) favor the magnetic-field-induced transformation in the D materials, while the protocols heat-apply (ha) and cool-remove (cr) favor the magnetic-field-induced transformation in the I materials.

is realized in the range of compositions $0.19 \leqslant x \leqslant 0.25$. For $x > 0.25$, T_t temperature is significantly larger than T_{c_M}. In the system $Ni_{2+x}Mn_{1-x-y}Ga_{1+y}$, where Mn is partially substituted by both Ni and Ga, one has another degree of freedom to adjust the transformation temperature closer to room temperature.[17–19] The alloy studied in this paper, $Ni_{53.3}Mn_{20.1}Ga_{26.6}$, has $x + y = 0.19$ and $y = 0.06$ giving a transition temperature $T_t = 322.4$ K which is slightly below $T_{c_A} = 337$ K (see Fig. 1).

Ni-Mn-Co-Sn *with inverse MCE*. Heusler alloys of the $Ni_2Mn_{1+y}Sn_{1-y}$ system can exhibit a peculiar phase transformation from the low-temperature paramagnetic martensite to a high-temperature ferromagnetic austenite[9] and, therefore, are characterized by an inverse MCE. The phase transformation sequence where $T_{c_M} < T_{c_A}$ is sketched in the right side of Fig. 1. In the off stoichiometric alloys, the substitution of Sn by Mn leads to an increase of the martensitic transformation temperature. In these alloys the high-temperature phase is $L2_1$ austenite and a low-temperature phase is tetragonal martensite with the 10M modulation. With $y = 0.48$ ($Ni_{50}Mn_{37}Sn_{13}$) the transition temperature is around room temperature. It takes place (according to the DSC peaks) on heating at 310 K (M to A) and on cooling at 295 K (from A to M).[9] Curie temperature of the martensitic phase, T_{c_M}, is equal to 230 K, while that of the austenitic phase $T_{c_A} = 311$ K. A small substitution of Co for Mn further reduces T_t and increases T_{c_A}.[10] The alloy studied in this paper, $Ni_{50}Mn_{36}Co_1Sn_{13}$, has a transition temperature at 295 K on heating and at 279 K on cooling and $T_{c_A} = 321$ K. The variation of the saturation magnetization between the two phases A and M is around $M_A - M_M = 40\ Am^2\ kg^{-1}$ and the entropy change at the transformation is around $s_A - s_M = 30\ J\ kg^{-1}\ K^{-1}$.[10,15]

Samples were prepared by the method described in Ref. 14. The $Ni_{53.3}Mn_{20.1}Ga_{26.6}$ single crystalline sample with a mass of 96.3 mg was about 6 mm long, and the lateral sides were around 1–2 mm. The magnetic field was applied along its longest direction. The $Ni_{50}Mn_{36}Co_1Sn_{13}$ polycrystalline sample with a mass of 49 mg had rectangular-like shape with characteristic dimension of about 2 mm. Both the samples had a flat side that was in the thermal contact with Peltier sensor of the calorimeter. A small quantity of thermal conducting paste was also used in order to improve the quality of the thermal contact.

Magnetization curves were measured by a SQUID magnetometer (Quantum Design MPMS-SS). Magnetization $M(H_a,T)$ as a function of temperature was measured under heating and cooling in the range of the martensitic phase transition. The applied magnetic field values were in the range 0.1–2.0 T.

Calorimetric measurements were preformed by Peltier cell calorimeter described in Ref. 15. We have measured the specific heat $c_p(H,T)$ at a constant applied magnetic field H by temperature scanning experiments on heating and cooling, as well as the entropy change $\Delta s(H,T)$ due to the change of H at a constant temperature T.[15] The temperature is changed at the rate of 50 mK s^{-1}. The accuracy of our Peltier calorimetry is ± 0.2 K for temperature, $\pm 3\%$ for the specific heat and for entropy, $\pm 2\%$ for dT/dH.

The isothermal experiments were performed employing four different protocols that realize all possible combination for the variation of the two variables in the (H,T) plane. The four possible combinations used for the measurements at a constant temperature are as follows (see Fig. 2):

(i) heat-apply (ha): (h) heating up to T starting from a full low-temperature (martensite) state at T_- with the magnetic field off $(0,T_- \rightarrow T)$; (a) applying the magnetic field at the constant temperature T $(0 \rightarrow H,T)$.

(ii) heat-remove (hr): (h) heating up to T starting from a full low-temperature state at T_- with the magnetic field on $(H,T_- \rightarrow T)$; (r) removing the magnetic field at the constant temperature T $(H \rightarrow 0,T)$.

(iii) cool-apply (ca): (c) cooling down to T starting from a full high-temperature (austenite) state at T_+ with the magnetic field off $(0,T_+ \rightarrow T)$; (a) apply the magnetic field at constant temperature $(0 \rightarrow H,T)$.

(iv) cool-remove (cr): (c) cooling down to T starting from a full high-temperature state at T_+ with the magnetic field on $(H,T_+ \rightarrow T)$; (r) remove the magnetic field at constant temperature $(H \rightarrow 0,T)$.

In materials with the direct MCE, the sequences (hr) and (ca) further advance the transformation, while (ha) and (cr) reverse its sign. The opposite situation occurs in materials with the inverse effect.

To find a relation between Δs obtained by changing H or changing T we model the phase transformation by taking the difference between the Gibbs free energy of the two phases $g_M - g_A$ as the equivalent force, where the Gibbs free energy

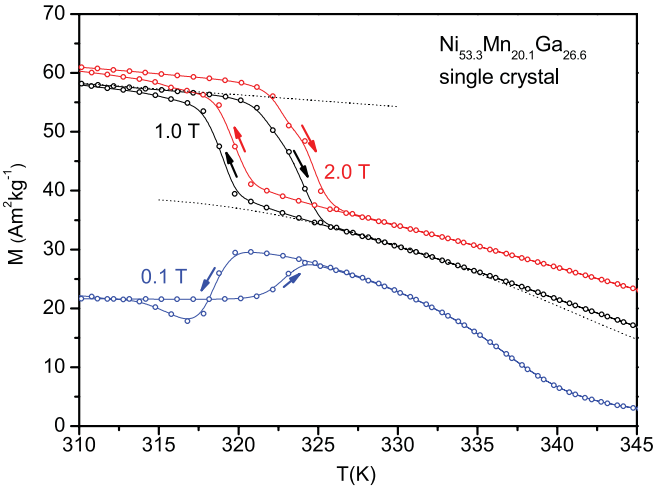

FIG. 3. (Color online) Magnetization of $Ni_{53.3}Mn_{20.1}Ga_{26.6}$ single crystal measured by changing temperature (heating and cooling) under constant applied magnetic field. (Dotted lines) Model [Eq. (4) and parameters in the text] for $\mu_0 H = 1$ T.

of the martensite g_M and the austenite g_A are both dependent on H and T.[16] By representing the phase fraction of austenite x_A as a function of $g_M - g_A$, we obtain a hysteresis plot where all the curves, measured by changing T at different H, rescale on the same loop. To determine the internal branching of hysteresis we also measured a set of partial transformations by changing T up to a peak value T_p in the middle of the transformation and then returning back.

III. EXPERIMENTAL RESULTS

The measured magnetization curves $M(H,T)$ are shown in Figs. 3 and 4 under magnetic fields of 0.1, 1.0, and 2.0 T. The change of magnetization with temperature, for 1.0 and 2.0 T,

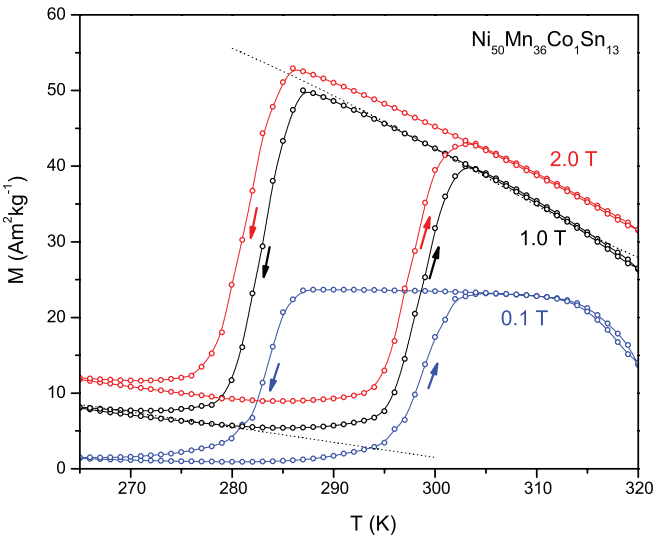

FIG. 4. (Color online) Magnetization of $Ni_{50}Mn_{36}Co_1Sn_{13}$ measured by changing temperature (heating and cooling) under constant applied magnetic field. (Dotted lines) Model [Eq. (4) and parameters in the text] for $\mu_0 H = 1$ T.

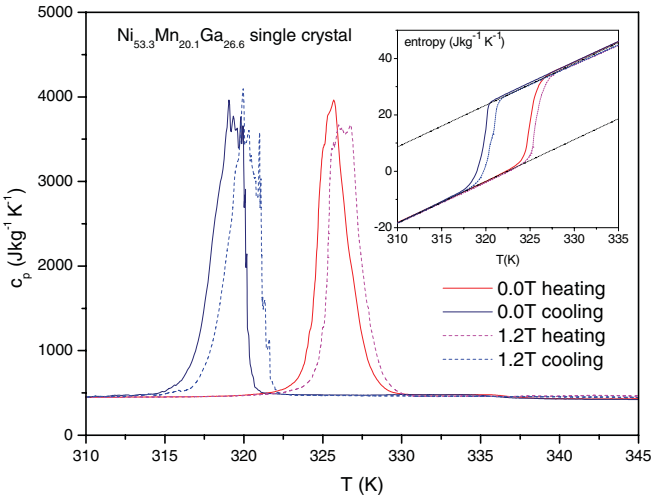

FIG. 5. (Color online) Specific heat of $Ni_{53.3}Mn_{20.1}Ga_{26.6}$ single crystal from heating and cooling temperature scans at 0.0 T and 1.2 T of applied magnetic field. (Inset) The entropy $s - s_0$, where s_0 is the entropy of M phase at $T_t = 322.4$ K. The dashed lines shows the entropy levels in the full M or A states: $s_M = 1.48 \times (T - T_t)$ J kg^{-1}K^{-1} and $s_A = 27.6 + 1.48 \times (T - T_t)$ J kg^{-1}K^{-1}.

reproduce well the change of magnetic order as expected from the scheme of Fig. 1, while the low field (0.1 T) behavior of the magnetization is influenced by the effect of demagnetizing field.

The specific heat $c_p(H,T)$ measured on heating and cooling temperature scans with and without applied magnetic field H is shown for the Ni-Mn-Ga and Ni-Mn-Co-Sn samples in Figs. 5 and 6, respectively. The value of the magnetic field was selected in order to have that the ratio of the peak temperature shift over the temperature hysteresis is approximately the

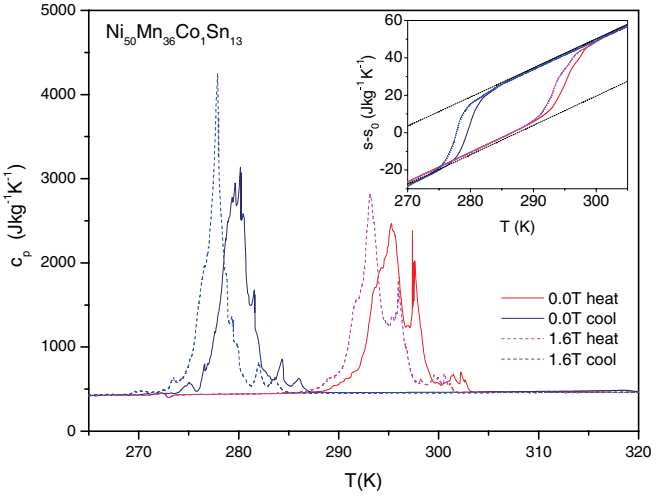

FIG. 6. (Color online) Specific heat of $Ni_{50}Mn_{36}Co_1Sn_{13}$ from heating and cooling temperature scans at 0.0 and 1.6 T of applied magnetic field. (Inset) The entropy $s - s_0$ where s_0 is the entropy of M phase at $T_t = 287.5$ K. The dashed lines shows the entropy levels in the full M or A states: $s_M = 1.57 \times (T - T_t)$ J kg^{-1}K^{-1} and $s_A = 30.7 + 1.55 \times (T - T_t)$ J kg^{-1}K^{-1}.

same for both samples. Specific heat demonstrates that the peaks corresponding to the martensitic phase transformation superimposed to the baseline specific heat: $c_p \simeq 470$ J kg^{-1} K^{-1} for Ni-Mn-Ga and $c_p \simeq 450$ J kg^{-1} K^{-1} for Ni-Mn-Co-Sn. In both samples the peaks have a noisy character that is mostly repeatable in different measurements. This effect is a consequence of the fact that the martensitic phase transformation proceeds through a sequence of avalanches.[20]

$Ni_{53.3}Mn_{20.1}Ga_{26.6}$ transforms from M to A on heating at 325.0 K and from A to M on cooling at 319.8 K (5.2 K of hysteresis width). The conventional transition temperature given by the average of the two value is $T_t = 322.4$ K. The magnetic field shifts the transition temperature at the rate $dT/d(\mu_0 H) = 0.7$ K T^{-1}. The entropy computed as in Ref. 15 is shown in the inset of Fig. 5, where s_0 is the entropy value on heating at T_t. The entropy change at the transition temperature is $s_A - s_M = 27.6$ J kg^{-1} K^{-1}, in good agreement with data available in the literature for similar alloys.[11]

$Ni_{50}Mn_{36}Co_1Sn_{13}$ transforms on heating from M to A at 295.3 K and on cooling from A to M at 279.7 K (15.6 K of hysteresis width). The conventional transition temperature, given by the average of the two is $T_t = 287.5$ K. With an applied magnetic field the phase transition temperatures decrease by -1.25 K T^{-1} because the magnetic field stabilizes the high-temperature phase (ferromagnetic austenite). The entropy, shown in the inset of Fig. 6, with the reference s_0 being the entropy value at T_t, gives a difference $s_A - s_M = 30.7$ J kg^{-1} K^{-1}.

The relative vertical position of the entropy at zero and at a given magnetic field H is determined by performing isothermal measurements of the entropy change $\Delta s(H,T_0) = s(H,T_0) - s(0,T_0)$ at a reference temperature outside the transition region. The magnetic-field-induced entropy change $\Delta s(H,T)$ shown in Fig. 7 and Fig. 8 as full lines is obtained by subtracting the entropy curves at different magnetic fields $\Delta s(H,T) = s(H,T) - s(0,T)$ separately on heating and cooling. The entropy change is characterized by high peaks at the transition temperatures, which is in agreement with previously published data (see, e.g., Ref. 9). To determine the reversibility or irreversibility of Δs in the transition region, we performed direct isothermal measurements by the application of the magnetic field on four measuring protocols in the (H,T) plane as described in Sec. II (see Fig. 2).

The measured isothermal entropy change $\Delta s(H,T)$ is shown in Fig. 7 for Ni-Mn-Ga and Fig. 8 for Ni-Mn-Co-Sn, respectively. In the figures, open symbols refer to measurements performed by the protocols advancing the transformation while full symbols are used for the protocols reversing the transformation. For Ni-Mn-Ga with the direct effect (D), the measurements with the protocols (hr) and (ca) reproduce the peak of the entropy change measured under heating and cooling, respectively. For Ni-Mn-Co-Sn with the inverse effect (I), this occurs for the (ha) and (cr) protocols. The entropy change determined on the protocols advancing the transformation (open symbol) is irreversible, i.e., it is obtained only the first time the magnetic field is changed (see the inset in Fig. 7). In order to achieve again the same Δs value one has to reset the experiment to the initial T_- or T_+ temperature and reapply the proper protocol. The entropy change obtained for the protocols reversing the transformation

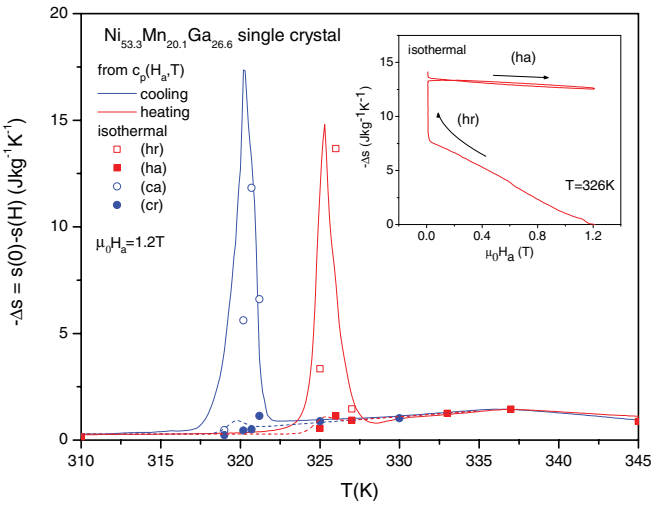

FIG. 7. (Color online) Entropy change of $Ni_{53.3}Mn_{20.1}Ga_{26.6}$ single crystal as a function of temperature. (Lines) Calculation from the differences between the experimental entropy curves (Fig. 5). (Points) Results of isothermal measurements for the heating (squares) and cooling (circles) protocols. (Inset) An isothermal measurement where the sample was heated up to $T = 326$ K in a magnetic field of $\mu_0 H = 1.2$ T, H was removed (hr), and then H was applied and removed again. The latter process resulted in a reversible minor hysteresis loop.

is found to be reversible, i.e., it is reproduced if the magnetic field is further changed back and forth (inset in Fig. 7), however, the Δs value is much smaller than the previous case. An interpretation of this big difference can be given by observing that (i) the protocols that advance the transformation drive the system along the saturation hysteresis loop of its

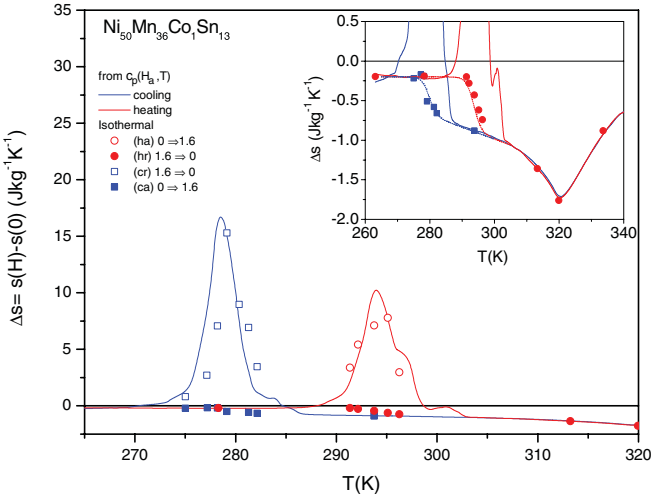

FIG. 8. (Color online) Entropy change of $Ni_{50}Mn_{36}Co_1Sn_{13}$ as a function of temperature. (Lines) Calculation from the differences between the experimental entropy curves (Fig. 6). (Points) Results of isothermal measurements for the heating (circles) and cooling (squares) protocols. (Inset) The same curve in a wider temperature range with the peak of MCE of at Curie temperature of austenite $T_{c_A} = 321$ K.

phase transformation while (ii) the protocols that reverse the transformation drive the system along a return hysteresis branch. Once the system is along a return branch a closed reversible minor loop is traced and the change in the phase fraction is much less than along the irreversible saturation loop. This effect depends on the amplitude of the driving force and on the width of the hysteresis of the phase transformation. The amplitude of the hysteresis in terms of magnetic field can be roughly evaluated as $\Delta H_{\rm hyst} = \Delta T_{\rm hyst}/(dT/dH)$ by considering the phase diagram of Fig. 2.[10] It is $\mu_0 \Delta H_{\rm hyst} \simeq 7$ T for the Ni-Mn-Ga single crystal and $\mu_0 H_{\rm hyst} \simeq 12$ T for the Ni-Mn-Co-Sn sample. However, with respect to Ref. 10, to understand the degree of the reversibility and irreversibility, we represent, by using a model, the phase transformation as a function of an equivalent driving force that summarizes the action of the magnetic field, H, and the temperature, T.

IV. MODEL

We consider the phase transition between the martensite (M) phase and the austenite phase (A) driven by either the temperature T or the applied magnetic field H. At thermodynamic equilibrium the system would select the state where the Gibbs free energy is minimum. Then, in presence of two phases M and A with different magnetic properties and Gibbs free energies g_M and g_A, respectively, the sign of the difference $g_M - g_A$ dictates which phase is stable: if $g_M - g_A < 0$, then the M phase is stable, whereas if $g_M - g_A > 0$, then the A phase is stable. When hysteresis is present, the system transforms from one phase to the other only if the difference between the energies overcomes a certain threshold value g_c, i.e., from A to M when $g_M - g_A < -g_c$ and from M to A when $g_M - g_A > g_c$. In the presence of a continuous phase transition characterized by a smooth change of the austenite phase fraction x_A and a distribution of threshold values, the difference $g_M - g_A$ plays the role of a driving force for the transformation summarizing the action of the temperature and the applied magnetic field.[13,16] The hysteresis behavior of a phase transformation can then be represented as the phase fraction x_A versus the driving force $g_M - g_A$.

To test this representation for our systems, we introduce the Gibbs free energy for each single phase i (M, A) given as

$$g_i(H,T) = f_i(T) - \mu_0 \int_0^H M_i(H,T) dH. \tag{1}$$

The first term on the right-hand side, $f_i(T)$, depends only on temperature. For temperatures around the transition temperature T_t it can be expressed by a second-order power expansion in $(T - T_t)$:,

$$f_i(T) = -s_{0_i}(T - T_t) - \tfrac{1}{2} b_i (T - T_t)^2, \tag{2}$$

where b_i is the specific entropy coefficient. The second term on the right-hand side is directly related to the magnetization of the pure phases. In order to have analytic expressions for g_i in the phase coexistence state, we choose a simplified description of the magnetization $M_i(H,T)$ of each single phase. We assume for $M(H,T)$ the behavior as shown in Fig. 9. For $H < H_{0_i}$ the linear law

$$M_i(H,T) = \chi_{0_i} \mu_0 H \tag{3}$$

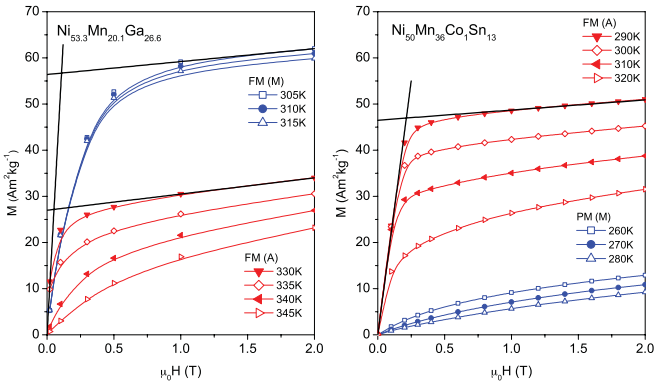

FIG. 9. (Color online) Magnetization measured outside the transition region. (Left) $Ni_{53.3}Mn_{20.1}Ga_{26.6}$ single crystal; (right) $Ni_{50}Mn_{36}Co_1Sn_{13}$. (Dotted lines) Model [Eq. (4) and parameters in the text] for $\mu_0 H = 1$ T.

represents the effect of the demagnetizing field and the presence of magnetic anisotropy. We then expect the coefficient χ_{0_i} to be almost independent of temperature. In the case of demagnetizing field the coefficient is $\chi_{0_i} = v/N_d$, where N_d is the demagnetizing factor and v is the specific volume. For $H > H_{0_i}$ the expression:

$$M_i(H,T) = M_{1_i}(T) + \chi_{1_i}(T) \mu_0 H, \tag{4}$$

where both M_{1_i} and χ_{1_i} depend on temperature, is a simplified description of a ferromagnet close to the Curie point. The threshold field H_{0_i} is defined as $\mu_0 H_{0_i} = M_{1_i}/(\chi_{0_i} - \chi_{1_i})$. H_{0_i} represents the typical field at which, in the single phases, there is a change in the magnetization process. For $H < H_{0_i}$ the magnetization process is related to magnetostatic energy and magnetic anisotropy, while for $H > H_{0_i}$ it is connected to the approach to magnetic saturation. The coefficient of the simplified expression for $M_i(H,T)$ of Eqs. (3) and (4), will be determined by the fit to the measured magnetization outside the transition region. The Gibbs free energy is

$$g_i(H,T) = f_{0_i}(T) - \tfrac{1}{2} \mu_0 \chi_{0_i} H^2 \tag{5}$$

for $H < H_{0_i}$ and

$$g_i(H,T) = f_{0_i}(T) - \mu_0 M_{1_i} H - \tfrac{1}{2} \mu_0 \chi_{1_i} H^2 + \tfrac{1}{2} \mu_0 M_{1_i} H_{0_i} \tag{6}$$

for $H > H_{0_i}$. The corresponding entropy for each phase is given by $s_i = -\partial g_i/\partial T$. By taking $d\chi_{0_i}/dT = 0$ we have

$$s_i = s_{0_i} + b_i (T - T_t) \tag{7}$$

for $H < H_{0_i}$ and

$$s_i = s_{0_i} + b_i (T - T_t) + \frac{dM_{1_i}}{dT} \mu_0 (H - H_{0_i}) + \frac{1}{2} \frac{d\chi_{1_i}}{dT} \mu_0 \left(H^2 - H_{0_i}^2\right) \tag{8}$$

for $H > H_{0_i}$. The parameters in Eqs. (7)–(8) can be determined by fit of the corresponding laws to the measured entropy and magnetization on both samples. By linear fit of the measured entropy (inset of Figs. 5 and 6) for $H = 0$ we obtain $s_M = 1.48 \times (T - T_t)$, $s_A = 27.6 + 1.48 \times (T - T_t)$ for Ni-Mn-Ga

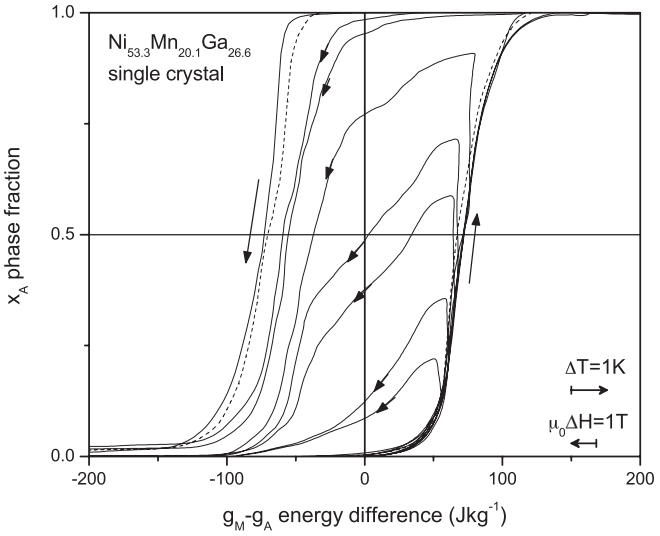

FIG. 10. Hysteresis of the phase transition of $Ni_{53.3}Mn_{20.1}Ga_{26.6}$ single crystal represented as the phase fraction of austenite x_A as a function of the energy difference $g_M - g_A$. Deduced from the experimental $s(H,T)$ curves.

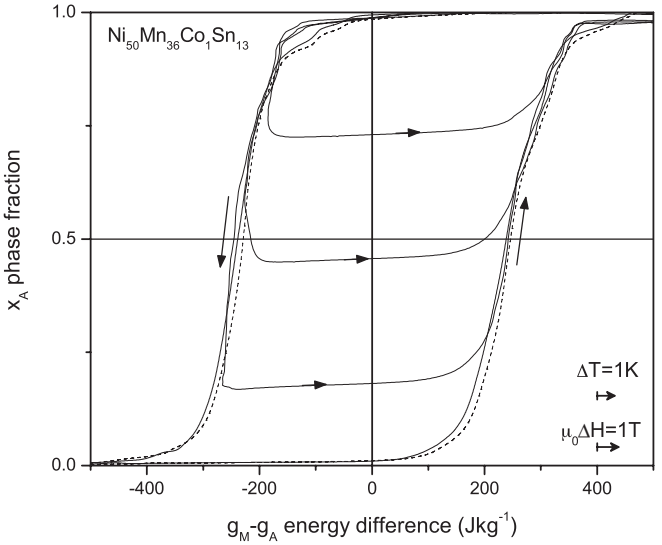

FIG. 11. Hysteresis of the phase transition of $Ni_{50}Mn_{36}Co_1Sn_{13}$ represented as the phase fraction of austenite x_A as a function of the energy difference $g_M - g_A$. Deduced from the experimental $s(H,T)$ curves.

and $s_M = 1.57 \times (T - T_t)$, $s_A = 30.7 + 1.55 \times (T - T_t)$ for Ni-Mn-Co-Sn. From the fit of Eqs. (3) and (4) to the data $M(H,T)$ outside the transition region, as shown in Fig. 9, we obtain the following: $\chi_{0_M} = 200$, $M_{1_M} = 53 - 0.2 \times (T - T_t)$, $\chi_{1_M} = 2.8$ and $\chi_{0_A} = 500$, $M_{1_A} = 33 - 0.6 \times (T - T_t) - 0.025 \times (T - T_t)^2$, $\chi_{1_A}^{-1} = 0.35 - 0.01 \times (T - T_t)$ for Ni-Mn-Ga and $\chi_{0_M} = 220$, $M_{1_M} = 0 - 0.2 \times (T - T_t)$, $\chi_{1_M} = 3.7$ and $\chi_{0_A} = 220$, $M_{1_A} = 48.5 - 0.7 \times (T - T_t) - 0.005 \times (T - T_t)^2$, $\chi_{1_A}^{-1} = 0.41 - 0.0085 \times (T - T_t)$ for Ni-Mn-Co-Sn. In the previous expressions the entropy s is measured in $\mathrm{J\,kg^{-1}K^{-1}}$, the magnetization M in $\mathrm{Am^2\,kg^{-1}}$ and the susceptibility χ in $\mathrm{Am^2\,kg^{-1}\,T^{-1}}$. We also verified that the same values of the parameters, used in Eq. (8), well describe the measured magnetic-field-induced entropy change of Figs. 7 and 8, out of the transition region.

From the values of χ_{0_i} the demagnetizing coefficient is estimated to be $N_d \simeq 0.2$ for Ni-Mn-Ga sample and $N_d \simeq 0.4$ for Ni-Mn-Co-Sn sample, coherently with the shape of the samples. The lower value of χ_{0_M} with respect to χ_{0_A} can be attributed to the magnetic anisotropy of the martensitic phase of Ni-Mn-Ga. The presence of magnetic anisotropy also explains why $M_M < M_A$ at the low field of 0.1 T of Fig. 3.

The phase fraction of the austenite phase, x_A, is computed from the measured entropy curves $s(H,T)$ by the equation

$$x_A = \frac{s - s_M}{s_A - s_M}, \tag{9}$$

where s_A and s_M are the entropies in the full A and M phases, respectively, of Eq. (7). The hysteresis plots shown in Figs. 10 and 11 are the plot of x_A as a function of $g_M - g_A$ computed by Eqs. (5) and (6):

$$\begin{aligned} g_M - g_A = &-\left(s_{0_M} - s_{0_A}\right)(T - T_t) - \tfrac{1}{2}(b_M - b_A)(T - T_t)^2 \\ &- \mu_0\left(M_{1_M} - M_{1_A}\right)H - \tfrac{1}{2}\mu_0\left(\chi_{1_M} - \chi_{1_A}\right)H^2 \\ &+ \tfrac{1}{2}\mu_0\left(M_{1_M}H_{0_M} - M_{1_A}H_{0_A}\right). \end{aligned} \tag{10}$$

For the applied magnetic field of our experiments, we find that the most important contributions to $g_M - g_A$ is due to the difference $M_{1_M} - M_{1_A}$ which is proportional to the difference in the spontaneous magnetization of the two phases. In the x_A versus $g_M - g_A$ plot we obtain that the curves measured without magnetic field (full lines) and with the magnetic field H (dashed lines) well rescale one over the other by using all the parameters determined by the magnetization measurements. As far as the process can be considered time independent or static, the presence of this rescaling proves the equivalent action of T and H on the phase transformation.

V. RETURN BRANCHES AND ENTROPY CHANGE

To characterize the material behavior for all the preparation protocols for which the transformation is reversed, hysteresis has to be completed by the knowledge of the return branches describing the internal behavior of the loop. For this aim, we measured a set of internal partial transformation by changing T. Temperature was changed at a constant rate of 50 $\mathrm{mK\,s^{-1}}$ up to the peak value T_p in the middle of the transformation and then the sign of the rate of change was inverted. The time taken by the control system to invert the rate of change is about 60 s. According to the Peltier cell method described in Ref. 15, the temperature of the sample T is lagging behind the temperature of the thermal bath T_b, which is controlled by the setup and kinetic corrections to the measured quantities are needed. In the transient around the turning point at T_p for the temperature of the thermal bath, the temperature of the sample T is given by $T = T_0 + v_P/\epsilon$, where v_P is the measured Peltier voltage and T_0 is the temperature of the empty reference cell. T_0 is given by the numerical integration of the equation $\tau dT_0/dt + T_0 = T_b(t)$ and the parameters ϵ and τ depend on the measuring cells and are determined according to the method described in Ref. 15.

In Figs. 10 and 11 the phase fraction of austenite phase x_A is plotted as a function $g_M - g_A$, as described in the previous section. The internal branching of the hysteresis qualitatively differ between the two samples. The return branches of Ni-Mn-Co-Sn are rather flat, which indicates that the interphase is rather blocked. In the return branches of Ni-Mn-Ga, after a small flat region, the phase boundaries can move more easily than in the case of Ni-Mn-Co-Sn. This difference can be related to the absence of grain boundaries in the single crystal.

A feature presented in both the measurements is the continuation of the phase transformation in the forward direction for the period of time needed to invert the direction of the temperature variation. This is seen as an almost vertical slope or a rounding of the tip of the return branch. The effect could be presumably attributed to an intrinsic time relaxation effect associated to the thermal activation of the structural and/or magnetic domains over their energy barriers. A similar phenomenon at the return branches tip was previously observed in the magnetization process of magnetic materials characterized by small correlation regions that can be thermally activated by spontaneous fluctuations.[21] The comprehension of this effect merits, however, further investigation.

VI. DISCUSSION

The knowledge of the hysteresis loop expressed by the equivalent driving force permits to derive the amplitude of the magnetic field needed to pass from one to the other of the two hysteresis branches. The major hysteresis loops for the two materials shown in Figs. 10 and 11 are well approximated by the function $x_A = (1/2)[1 + \tanh(\Delta g \pm g_c)/g_0]$ with $g_c = 75\ \mathrm{J\,kg^{-1}}$, $g_0 = 20\ \mathrm{J\,kg^{-1}}$ for Ni-Mn-Ga and $g_c = 240\ \mathrm{J\,kg^{-1}}$, $g_0 = 70\ \mathrm{J\,kg^{-1}}$ for Ni-Mn-Co-Sn, $\Delta g = g_M - g_A$. The width of the hysteresis loop is a measure of the typical energy barriers associated with the processes of nucleation and growth that ultimately depend on the elastic energy accumulated at the interface between martensite and austenite phases.[22]

The linear reversible permeabilities along the return branches are approximately $\Delta x_A = \Delta g / g_{\mathrm{rev}}$ with the parameter for Ni-Mn-Ga initially $g_{\mathrm{rev}} = 1200\ \mathrm{J\,kg^{-1}}$ and in the middle $g_{\mathrm{rev}} = 250\ \mathrm{J\,kg^{-1}}$ and for Ni-Mn-Co-Sn $g_{\mathrm{rev}} = 2 \times 10^4\ \mathrm{J\,kg^{-1}}$. The reversible permeability reflects the possibility to have reversible motion of the interfaces once they are nucleated.

To evaluate the performance of the material as an heat exchanger using the magnetocaloric effect at the first-order phase transition, we compare the measured reversible entropy change with the correspondent change of the phase fraction along the return branches. An applied magnetic field variation of 1.2 T for Ni-Mn-Ga corresponds to $\Delta g \simeq 25\ \mathrm{J\,kg^{-1}}$ while a variation of 1.6 T for Ni-Mn-Co-Sn to $\Delta g \simeq 65\ \mathrm{J\,kg^{-1}}$ (see the arrows in Figs. 10 and 11). With these numbers the variation of the phase fraction along the return branches is $\Delta x_A \simeq 1.8 \times 10^{-2}$ for Ni-Mn-Ga and $\Delta x_A \simeq 3 \times 10^{-3}$ for Ni-Mn-Co-Sn. In a phase transition region the entropy is $s = x_A s_A + x_M s_M$ ($x_A + x_M = 1$) and its change is given by the sum of three terms

$$\Delta s = x_A \Delta s_A + (1 - x_A)\Delta s_M + (s_A - s_M)\Delta x_A. \quad (11)$$

The first two terms are the magnetocaloric contribution of the phases while the third is contribution of the phase transformation. The third term contributes as $\Delta s = 0.5\ \mathrm{J\,kg^{-1}\,K^{-1}}$ for Ni-Mn-Ga and $\Delta s \simeq 0.09\ \mathrm{J\,kg^{-1}\,K^{-1}}$ for Ni-Mn-Co-Sn. If we compare these values with the measured reversible entropy change it turns out that for Ni-Mn-Co-Sn the contribution of phase transition is negligible and in Ni-Mn-Ga is appreciable but less than the magnetocaloric contribution of the single phases. The corresponding entropy change with the three contributions is shown in Fig. 7 and in the inset of Fig. 8 as a dashed curve. It is evident that the behavior of the reversible entropy change as a function of temperature is well reproduced.

VII. CONCLUSION

In this work we have investigated the magnetocaloric effect along the hysteresis in the phase transformation of Heusler alloys of interest for room-temperature magnetic refrigeration. Although the Heusler alloys have a large entropy change at the magnetostructural transition, it is shown that the giant MCE can be obtained only under the measuring protocols in which the magnetic field further advance the transformation initiated by the temperature change.[10] This large MCE originates from a contribution of the structural subsystem and is largely irreversible for the typical magnetic fields available with electromagnets.

We have introduced a model to represent the measured entropy in terms of the phase fraction of the austenite x_A as a function of the driving force give by the difference between the Gibbs free energy of the two phases $g_M - g_A$. This plot allows us to rescale all data within a unified picture in which the impact of both the magnetic field H and the temperature T on the phase transformation with hysteresis can be understood. By using the hysteresis loops and the return branches one can link magnitude of the attainable entropy change to the hysteresis of the phase transition. The hysteresis loops and return branches give the possibility to predict behavior of the magnetic entropy change on a variety of measurement protocols.

For the studied materials, $Ni_{53.3}Mn_{20.1}Ga_{26.6}$ and $Ni_{50}Mn_{36}Co_1Sn_{13}$, the full phase transition by the magnetic field can occur only for elevated magnitudes of H. An estimation based on the developed model indicates (i) both the strength of the magnetic field necessary for the pass from one hysteresis branch to the other, estimated as $\mu_0 H_{\mathrm{hyst}} = 2g_c/\Delta M$, is $\mu_0 H_{\mathrm{hyst}} \geqslant 7$ T for the Ni-Mn-Ga single crystal and $\mu_0 H_{\mathrm{hyst}} \geqslant 12$ T for the Ni-Mn-Co-Sn, in agreement with Ref. 10, and the contribution to the entropy change from the internal hysteresis branching, which turns out to differ somewhat between the two investigated samples. Our study, however, indicates that interesting developments are expected by the possibility of tuning the hysteresis in the structural phase transition.[23,24]

ACKNOWLEDGMENTS

Funding from the European Community's 7th Framework Programme under Grant No. 214864 (project SSEEC) is acknowledged. V.V.K. acknowledges the Creation and Development Program of NUST "MISiS" for financial support.

[1] A. Planes, L. Manosa, and M. Acet, J. Phys. Condens. Matter **21**, 233201 (2009).
[2] P. Egolf (ed.), *in proceedings of the Third IIF-IIR Int. Conf. on Magnetic Refrigeration at Room Temperature*, *Refrigeration Science and Technology Proceedings No. 2009-3* (International Institute of Refrigeration, Paris, 2009).
[3] V. K. Pecharsky and K. A. Gschneidner Jr., Phys. Rev. Lett. **78**, 4494 (1997).
[4] A. Fujita, K. Fukamichi, J.-T. Wang, and Y. Kawazoe, Phys. Rev. B **68**, 104431 (2003).
[5] E. Bruck, O. Tegus, D. T. Cam Thanh, Nguyen T. Trung, and K. H. J. Buschow, Int. J. Refrig. **31**, 763 (2008).
[6] A. N. Vasiliev, A. D. Bozhko, V. V. Khovailo, I. E. Dikshtein, V. G. Shavrov, V. D. Buchelnikov, M. Matsumoto, S. Suzuki, T. Takagi, and J. Tani, Phys. Rev. B **59**, 1113 (1999).
[7] V. V. Khovailo, V. Novosad, T. Takagi, D. A. Filippov, R. Z. Levitin, and A. N. Vasilev, Phys. Rev. B **70**, 174413 (2004).
[8] V. V. Khovaylo, K. P. Skokov, Yu. S. Koshkidko, V. V. Koledov, V. G. Shavrov, V. D. Buchelnikov, S. V. Taskaev, H. Miki, T. Takagi, and A. N. Vasiliev, Phys. Rev. B **78**, 060403(R) (2008).
[9] T. Krenke, M. Acet, E. F. Wassermann, X. Moya, L. Manosa, and A. Planes, Phys. Rev. B **72**, 014412 (2005).
[10] V. V. Khovaylo *et al.*, Phys. Rev. B **81**, 214406 (2010).
[11] C. P. Sasso, M. Kuepferling, L. Giudici, V. Basso, and M. Pasquale, J. Appl. Phys. **103**, 07B306 (2008).
[12] J. D. Zou, B. G. Shen, B. Gao, J. Shen, and J. R. Sun, Adv. Mater. **21**, 693 (2009).
[13] P. J. Shamberger and F. S. Ohuchi, Phys. Rev. B **79**, 144407 (2009).
[14] V. V. Khovaylo, K. P. Skokov, O. Gutfleisch, H. Miki, R. Kainuma, and T. Kanomata, Appl. Phys. Lett. **97**, 052503 (2010).
[15] V. Basso, C. P. Sasso, and M. Küpferling, Rev. Sci. Instrum. **79**, 063907 (2010).
[16] V. Basso, C. P. Sasso, and M. Lo Bue, J. Magn. Magn. Mater. **316**, 262 (2007).
[17] F. X. Hu, B. G. Shen, J. R. Sun, and G. H. Wu, Phys. Rev. B **64**, 132412 (2001).
[18] F. Albertini, L. Pareti, A. Paoluzi, L. Morellon, P. A. Algarabel, M. R. Ibarra, and L. Righi, Appl. Phys. Lett. **81**, 4032 (2002).
[19] X. Zhou, W. Li, H. P. Kunkel, and G. Williams, J. Phys. Condens. Matter **16**, L39 (2004).
[20] J. Ortin, A. Planes, and L. Delaey, in *The Science of Hysteresis*, edited by G. Bertotti and I. Mayergoyz (Elsevier, Amsterdam, 2006), Vol. III, p. 467.
[21] V. Basso, C. Beatrice, M. LoBue, P. Tiberto, and G. Bertotti, Phys. Rev. B **61**, 1278 (2000).
[22] M. Stipcich, L. Manosa, A. Planes, M. Morin, J. Zarestky, T. Lograsso, and C. Stassis, Phys. Rev. B **70**, 054115 (2004).
[23] R. D. James and Z. Zhang, in *Magnetism and Structure in Functional Materials*, edited by L. Manosa, A. Planes, and A. Saxena, Springer Series in Materials Science, Vol. 79 (Springer-Verlag, Berlin, 2005), p. 179.
[24] J. Cui *et al.*, Nat. Mater. **5**, 286 (2006).